C-26 and C-30 Apocarotenoids from Seeds of *Ditaxis heterantha* with Antioxidant Activity and Protection against DNA Oxidative Damage

María D. Méndez-Robles,[†] Herry H. Permady,[†] María E. Jaramillo-Flores,*[,†] Eugenia C. Lugo-Cervantes,[‡] Anaberta Cardador-Martínez,[‡] Alejandro A. Canales-Aguirre,[‡] Fernando López-Dellamary,[§] Carlos M. Cerda-García-Rojas,*[,∥] and Joaquín Tamariz[⊥]

Departamento de Alimentos, Escuela Nacional de Ciencias Biológicas, Instituto Politécnico Nacional, Prol. Carpio y Plan de Ayala, 11340 México, D. F., Mexico, Centro de Investigación y Asistencia en Tecnología y Diseño del Estado de Jalisco, Mexico, Departamento de Quimica de la Madera, Universidad de Guadalajara, Mexico, Departamento de Química, Centro de Investigación y de Estudios Avanzados del Instituto Politécnico Nacional, México, D. F. 07000, Mexico, and Departamento de Química Orgánica, Escuela Nacional de Ciencias Biológicas, Instituto Politécnico Nacional, Prol. Carpio y Plan de Ayala, 11340 México, D. F., Mexico

Received November 24, 2005

The hexane extracts of seeds of *Ditaxis heterantha* afforded two new apocarotenoids whose structures corresponded to methyl 3-oxo-12′-apo-ϵ-caroten-12′-oate (**1**) (heteranthin) and methyl 3β,6β-epoxy-5β-hydroxy-4,5-dihydro-8′-apo-ϵ-caroten-8′-oate (**2**) (ditaxin). Both compounds were evaluated for antioxidant activity and protection against DNA oxidative damage by using DPPH• free radical scavenging and Comet assays, respectively.

Carotenoids are composed of isoprene units, whose conjugated double bonds are responsible for their distinctive color. Most of the structural variations of carotenoids are found in the rings, whose double bonds are sensitive to oxidation, leading to the formation of apocarotenoids. For a symmetrical carotenoid, such as β-carotene, there are nine possible outcomes of a single bond scission due to oxidation. Apocarotenoid formation may be the result of nonspecific mechanisms such as lipoxygenase oxidation and photo-oxidation, as well as of specific mechanisms where particular dioxygenases operate in the formation of compounds such as vitamin A,[1] abscisic acid,[2] aromatic compounds,[3] and pigments.[4]

Several apocarotenoids have economic importance as pigments, as well as flavor and aroma compounds in a variety of foods, as is the case for bixin. This carotenoid is found on the cover of *Bixa orellana* seeds, and it is the product of the rupture of the lycopene molecule.[5] Similarly, crocetin is an apocarotenoid that originates in the rupture of zeaxanthin, a carotenoid found in the pistils of *Crocus sativus*.[6]

On the basis of extensive epidemiological observation, fruits and vegetables that are rich in carotenoids are thought to provide health benefits by decreasing the risk of various diseases, particularly certain cancers.[7−9] In part, the beneficial effects of carotenoids are thought to be due to their role as antioxidants. In vitro studies such as the TEAC (Trolox equivalent antioxidant capacity) test, radical [2,2-diphenyyl-1-picrylhydrazyl (DPPH•)] scavenging activity, and the oxygen radical absorbance capacity (ORAC) assay[10−12] have documented the capacity of carotenoids to quench free radicals by mechanisms that include addition of the radical to the carotenoid, hydrogen abstraction, and/or electron transfer. Those carotenoids with nine or more conjugated double bonds are able to quench singlet oxygen with increasing activity depending on the number of conjugated double bonds with lycopene (11 conjugated and two nonconjugated double bonds), being the most effective quencher of singlet oxygen.[13]

It has been indicated that the induction of oxygen radicals is clearly related to genotoxic events. Primary DNA damage in cells is an important end-point for the chemoprevention of carcinogenesis. In this context, the Comet assay has been used as a rapid and sensitive tool for detecting primary DNA damage in individual cells. This technique allows the detection of several classes of DNA injury such as double-strand breaks, single-strand breaks, alkali-labile sites, incomplete repair of a-basic sites, and cross-links.[14,15] There are some natural compounds, such as quercetin and α-tocoferol, that have already shown their ability to protect lymphocyte DNA against hydrogen peroxide treatment in the Comet assay.[16] Consequently, a decrease in DNA damage upon carotenoid intervention might be interpreted as a decrease in chronic diseases risk.

Ditaxis heterantha is a native plant of Mexico that grows in semiarid zones and belongs to the Euphorbiaceae family.[17,18] Its seeds have been used locally as a natural food flavor and coloring, and they have properties similar to saffron.[19] The seed's endosperm contains a yellow pigment characteristic of the carotenoid family. Detection of antioxidant activity could increase the value of *D. heterantha* as a food additive, expanding its market. Therefore, the aim of the present work is to elucidate the structure of the two main compounds of *D. heterantha* seed pigment, as well as to determine their antioxidant and antigenotoxic activities.

Results and Discussion

Compounds **1** and **2** were characterized by using a combination of 1- and 2-D NMR spectroscopy, including COSY, HMQC, HMBC, and NOESY experiments, in conjunction with mass spectrometry.

Apocarotenoid **1** (Figure 1) was obtained from fraction 4 as a yellow, amorphous powder, mp 120−122 °C, with $[\alpha]^{23}_{D}$ −669.8. The conjugated polyene system was suggested by its UV−vis absorption maxima at 237, 283, 323, 359, and 405 nm. Its IR spectrum indicated the presence of two absorptions for conjugated carbonyl groups (1704 and 1665 cm^{-1}). The strong band at 1233 cm^{-1} suggested the presence of one of the carbonyl groups as an ester group. The molecular formula, $C_{26}H_{34}O_3$, was inferred from the $[M]^+$ peak at *m*/*z* 394 in the MS spectrum and confirmed by HRMS, while the number of carbon atoms was supported by analysis of the ^{13}C NMR spectrum. The ^1H and $^1H-^1H$ COSY spectra of **1** (Table 1) revealed that this compound is an apocarotenoid. The ^1H NMR spectrum showed four singlets at δ 0.99, 1.06, 1.93, and 2.00, integrating for 3H each, assigned to Me-16, Me-17, Me-19, and Me-20, respectively. Unlike Me-19 and Me-20, where the allylic couplings were too small to be resolved into

* To whom correspondence should be addressed. Tel: (52) 55-5729-6000, ext. 62464. Fax: (52) 55-5729-6000, ext. 62359. E-mail: Jaramillo_flores@hotmail.com.
† Alimentos-ENCB-IPN.
‡ CIATEJ-Mexico.
§ UDG-Mexico.
∥ Quimica-CINVESTAV-Mexico.
⊥ Quimica Organica-ENCB-IPN.

10.1021/np050489f CCC: $33.50
Published on Web 07/22/2006

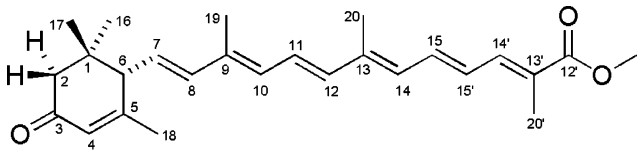

1

Figure 1. Apocarotenoid **1** structure.

Table 1. ^{1}H NMR (300 MHz) Chemical Shifts (ppm), Multiplicities, and Coupling Constants (Hz) of Apocarotenoids **1** and **2**[a]

1 proton	δ multiplicity (coupling constant)	**2** proton	δ multiplicity (coupling constant)
2α	2.10 d (16.9)	2α	1.40 d (11.5)
2β	2.38 d (16.9)	2β	1.79 ddd (11.5, 5.6, 2.2)
4	5.91 br s	3	4.47 dd (6.3, 5.6)
6	2.61 br d (9.3)	4α	1.70 d (12.9)
7	5.57 dd (15.2, 9.3)	4β	2.10 (12.9, 6.3, 2.2)
8	6.22 d (15.2)	7	5.74 d (15.6)
10	6.16 br d (11.3)	8	6.46 d (15.6)
11	6.67 dd (15.0, 11.3)	10	6.26 br d (10.8)
12	6.37 d (15.0)	10′	7.29 dd (10.8, 1.5)
14	6.26 br d (11.7)	11	6.61 m
14′	7.29 br d (11.7)	11′	6.50 dd (15.2, 10.8)
15	6.88 dd (14.2, 11.7)	12	6.36 d (14.2)
15′	6.53 dd (14.2, 11.7)	12′	6.61 d (15.2)
16	0.99 s	14	6.20 br d (11.2)
17	1.06 s	14′	6.36 d (10.8)
18	1.91 d (1.5)	15	6.67 m
19	1.93 s	15′	6.71 dd (14.2, 10.8)
20	2.00 s	16	1.25 s
20′	1.99 d (1.0)	17	0.91 s
CO_2CH_3	3.77 s	18	1.49 s
		19	1.99 d (1.0)
		19′	1.96 s (*)
		20	1.97 s (*)
		20′	1.97 s (*)
		CO_2CH_3	3.76 s
		OH	2.49 s

[a] Values marked with an asterisk may be interchanged.

doublets, Me-18 and Me-20′ appeared as doublets at δ 1.91 (1H, d, J = 1.5 Hz) and 1.99 (1H, d, J = 1.0 Hz), showing the allylic coupling with protons H-4 and H-14′, respectively. The AB system at δ 2.10 and 2.38 (each 1H, d, J = 16.9 Hz) corresponded to the geminal H-2β and H-2α, respectively. The *syn* relationship of H-2β and H-2α with regard to Me-17 and Me-16 was established by correlations in the NOESY experiment. The resonance of the bis-allylic H-6 was located at δ 2.61 (1H, br d, J = 9.3 Hz), which couples with H-7. This coupling is also found in the signal of the latter proton as a doublet of doublets at δ 5.57 (1H, dd, J = 15.2, 9.3 Hz). The larger coupling constant is due to the *trans* coupling with H-8. The signal of the latter appears at δ 6.22 (1H, d, J = 15.2 Hz) as a sharp doublet, since there is no other significant coupling with vicinal protons. The conformation of the polyene chain with respect to the cyclohexenone ring avoids the coupling between H-6 and H-8. In the vinylic proton region, the signals due to H-10, H-14, and H-14′ at δ 6.16 (1H, br d, J = 11.3 Hz), 6.26 (1H, br d, J = 11.7 Hz), and 7.29 (1H, br d, J = 11.7 Hz), respectively, clearly showed large coupling with their vicinal σ-bonded vinylic CH group. The broadness of these signals is due to the small residual coupling with the allylic proton. H-14′ is deshielded due to conjugation with the methoxycarbonyl group. Also in this region, there are three signals at δ 6.53 (1H, dd, J = 14.2, 11.7 Hz), 6.67 (1H, dd, J = 15.0, 11.3 Hz), and 6.88 (1H, dd, J = 14.2, 11.7 Hz), with a similar coupling pattern, a doublet of doublets, both with large coupling constants. These are attributed to H-15′, H-11, and H-15, respectively, which show a *trans* double bond coupling (average J = 14.5 Hz) and a three-bond σ CH−CH coupling (average J = 11.6 Hz). H-4 resonates as a broad singlet at δ 5.91 (1H, br s) as a consequence of the long-range coupling

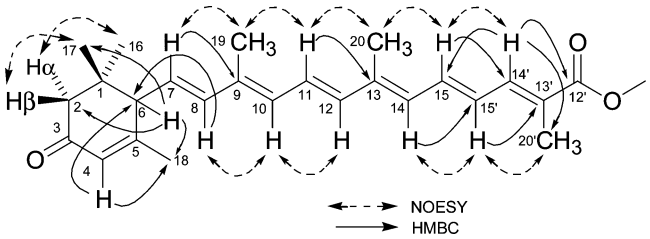

Figure 2. Selected NOESY and HMBC correlations in compound **1**.

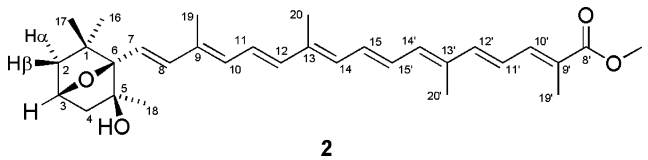

2

Figure 3. Apocarotenoid **2** structure.

Table 2. ^{13}C NMR (75.4 MHz) Chemical Shifts (ppm) of Apocarotenoids **1** and **2**[a]

carbon	**1**	**2**	carbon	**1**	**2**
1	37.0	41.5	12′	168.0	143.9
2	47.8	48.5	13	139.0	137.7
3	198.1	74.4	13′	126.0	135.4
4	125.2	49.1	14	131.2	131.8
5	161.4	80.1	14′	138.2	135.7
6	56.6	95.8	15	135.2	125.4
7	125.8	121.1	15′	127.8	131.9
8	137.8	136.6	16	27.9	26.3
8′		168.8	17	28.4	31.9
9	135.0	134.9	18	24.2	22.7
9′		125.8	19	13.7	12.9 (*)
10	131.2	132.0	19′		12.9 (*)
10′		139.0	20	13.4	12.7 (*)
11	125.6	129.4	20′	13.5	12.7 (*)
11′		123.1	CO_2CH_3	52.1	51.8
12	137.2	137.6			

[a] Values marked with an asterisk may be interchanged.

with Me-18. The positions of Me-19, Me-20, and Me-21′ were established by NOESY experiments, since a correlation of H-11 with both former methyl groups was observed, in addition to the correlation between Me-20 and H-15, while Me-20′ correlates with the signal attributed to proton H-15′ (Figure 2). The *syn* relationship between H-2α and H-2β, and Me-16 and Me-17, respectively, was confirmed by the NOESY spectrum. In agreement with the above ^{1}H NMR data, the ^{13}C NMR spectrum (Table 2) exhibited signals for two carbonyl groups (δ 198.1 and 168.0), along with 10 vinylic protonated carbons. The latter and those of the cyclohexenone moiety were assigned by HMQC. In the HMBC spectrum (Figure 2), H-14′ (δ 7.29) showed three-bond correlations with the carbonyl carbon at δ 168.0, with Me-20′ (δ 13.5), and with C-15 (δ 135.2). H-6 (δ 2.61) correlates with C-2, C-17, and C-18. C-6 (δ 56.6) correlates with H-4 and H-8, indicating that this carbon is part of the cyclohexenone ring and is bonded to the polyene chain. The signals due to the quaternary carbons C-9, C-13, and C-13′ were asigned as observed in the HMBC spectra, showing three-bond correlations with H-7, H-11, and H-15′, respectively.

Fraction 5 afforded compound **2** (Figure 3) as an orange, amorphous powder with $[\alpha]^{23}_D$ −117.0 ($CHCl_3$; *c* 0.02). The UV−vis spectrum shows absorption maxima at 227, 280, 322, 396, 418, and 459 nm. The first four bands suggested a similar conjugated polyene chain as shown in apocarotenoid **1**, but the last two absorptions indicate the presence of a longer conjugated system. In contrast with compound **1**, the IR spectrum showed the presence of a single absorption in the region of conjugated carbonyl groups (1702 cm^{-1}). The strong band at 3448 cm^{-1} indicates the presence of a non-hydrogen-bonded hydroxyl group. The molecular formula

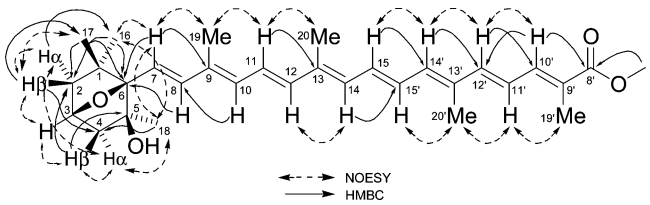

Figure 4. Selected NOESY and HMBC correlations in compound **2**.

of compound **2** was confirmed to be $C_{31}H_{42}O_4$ by the HRMS (FAB), showing a $[M]^+$ peak at *m*/*z* 478.3084.

The ^1H and ^{13}C resonances in the 1- and 2-D NMR spectra of **2** were assigned in a way similar to those of **1**. The NMR data (Tables 1 and 2) of the polyene part of ditaxin (**2**) were close to those of **1**, but additional vinylic proton and carbon signals were observed. In the alyphatic region of the ^1H NMR spectrum, apart from the singlets due to the methyl groups, only four signals were present: two doublets at δ 1.40 (1H, d, $J = 11.5$ Hz) and 1.70 (1H, d, $J = 13.2$ Hz), corresponding to the *endo* H-2α and H-4α with a large geminal coupling, and, as expected, the coupling with the bridgehead proton H-3 was absent. The signals attributed to the *exo* H-2β and H-4β at δ 1.79 (1H, ddd, $J = 11.5, 5.6, 2.2$ Hz) and 2.10 (1H, ddd, $J = 12.9, 6.3, 2.2$ Hz), respectively, consisted of a double doublet of doublets each. The largest coupling is ascribed to the geminal coupling, while the medium coupling is due to the coupling of these protons with the bridgehead H-3. The smallest coupling is the result of the *W* coupling between H-2β and H-4β, as shown in the COSY spectrum. Therefore, the doublet of doublets at δ 4.47 (1H, dd, $J = 6.3, 5.6$ Hz) corresponded to H-3. Its chemical shift is consistent with a proton bonded to a carbon of an ether group. In the vinylic region of the ^1H and $^1H-^1H$ COSY spectra of **2** (Table 1), the signals of the side-chain protons appear with the expected coupling in accordance with the number of their adjacent protons. Some of them appear as slightly broadened, resulting from the allylic or dienylic couplings. The lower field shift of the H-10′ signal (δ 7.29) indicated the bonding site of the closest conjugated double bond to the methoxycarbonyl group. On the other hand, high-field shifts of vinylic C-7 and H-7 are due to the fact that this carbon is attached to the sp^3 bridgehead C-6.

Characteristic correlations observed in the NOESY and HMBC experiments are shown in Figure 4. It is interesting to notice that in the NOESY spectra a correlation is found between H-7 and *endo* Me-16 and Me-18, suggesting a conformational preference of the polyene chain around the C-6/C-7 bond, in which H-7 is oriented downward and the double bond upward, *syn* to the oxa bridge. The *exo* position of Me-17 was also established by its NOE correlation with proton H-2β. In the HMBC spectrum, H-4β (δ 2.10) showed a C−H two-bond correlation with the quaternary C-5 (δ 80.1), which is bearing the hydroxyl group. Couplings between H-7 (δ 5.74) and H-8 (δ 6.46) with C-6 (δ 95.8) as well as a correlation between the latter with the singlets at δ 0.91 and δ 1.49 assigned to methyl groups Me-17, Me-16, and Me-18, respectively, confirmed the connectivity of the groups around C-6 (Figure 4).

Comparison of the specific rotation of the new apocarotenoids (**1** and **2**) with those of related molecules[20] allowed us to suggest that their absolute configuration is as depicted in Figures 1 and 3, respectively.

Results of an antiradical activity assay showed that the extract and compounds **1** and **2** have antioxidant activity comparable to that of astaxanthin at concentrations of 150 and 750 μM and 150 μM β-carotene (Figure 5). Antiradical activity increased as the test concentration increased from 150 μM to 1050 μM for all carotenoids assayed ($R \geq 0.88$, $p \leq 0.001$ by Pearson correlation). As expected, lycopene showed higher activity than the other carotenoids tested, except for astaxanthin, at 1500 μM (52%). Lycopene, because of its high number of conjugated dienes, is the most potent singlet oxygen quencher among the natural carotenoids.[13,21] The relative singlet oxygen quenching ability of a given carotenoid is based on the number of conjugated double bonds, and the terminal ionone ring of β-carotene (and related carotenoids) has no effect.[20] Apocarotenoid **2** has eight conjugated double bonds, while **1** has only six; therefore it was not surprising to find higher antioxidant activity for **2**. β-Carotene (1500 μM) showed an antiradical activity similar to that of lycopene (36%). [22] Compounds **1** (21%) and **2** (12%), as well as the extract (18%), have an even poorer scavenging ability than β-carotene and lycopene. Among the carotenoids of *D. heterantha*, compound **2** has the highest activity, followed by the extract and finally **1** ($p = 0.05$). The in vivo biological properties of the carotenoids may be much more related to the products of the interaction of carotenoids with oxidant stress, that is, breakdown products such as apocarotenoids and retinoids.[23,24] Apocarotenoids from *D. heterantha* could be a good source of antioxidants for consumers.

The protection of *D. heterantha* extracts against DNA oxidative damage was assessed in rat lymphocytes using the Comet assay. The viability of blood cells in all the samples was found to be in the range 90−95% (data not shown). The results of the Comet assay showed that the extract and compounds **1** and **2** have antigenotoxic activity. The Table 3 shows that lymphocytes exposed to hydrogen peroxide and without treatment (active compounds of *D. heterantha*) showed a significant increase in all the parameters of the Comet assay. Heteranthin and ditaxin at 1000 μM lead to a significant decrease in H_2O_2-induced DNA oxidative damage, while 500 μM showed lower protection (Table 3). Thus, both active compounds of *D. heterantha* protected the lymphocyte blood cells from the genotoxic damage in a dose-dependent manner. In recent years, attention has been focused on whether naturally occurring com-

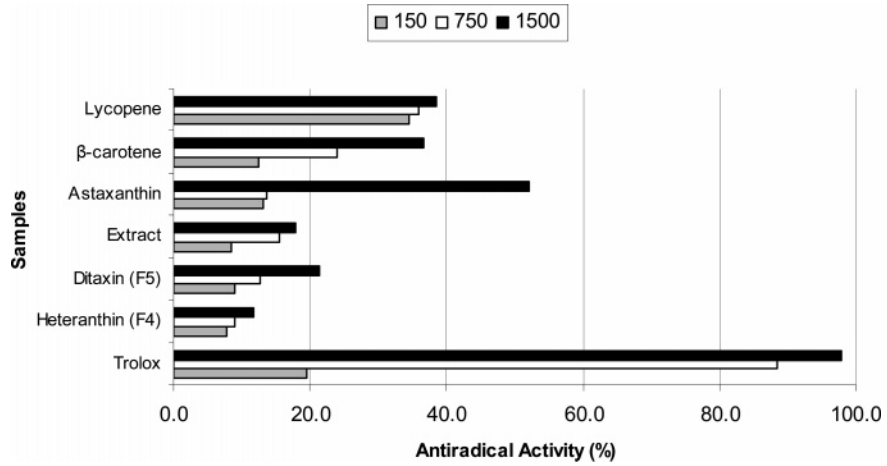

Figure 5. Antiradical activity of *D. heterantha* carotenoid extract, heteranthin (**1**), and ditaxin (**2**) as compared to carotenoid standards.

Table 3. Protection against Oxidative DNA Damage Effect of Ditaxin, Heteranthin, and *D. heterantha* Seed Extract by Comet Assay at Different Concentrations[a]

sample	tail moment cauda	tail moment olive	tail length
H_2O_2	24.67 ± 1.30	15.69 ± 0.65	37.14 ± 1.42
control	0.65 ± 0.12	0.86 ± 0.11	5.96 ± 0.59
extr/1000 μM	6.19 ± 1.18	4.52 ± 0.68	16.58 ± 1.98
extr/500 μM	7.37 ± 1.21	5.63 ± 0.78	17.58 ± 2.15
ditaxin/1000 μM	12.27 ± 1.32	8.21 ± 0.74	28.15 ± 1.90
ditaxin/500 μM	18.80 ± 1.57	11.58 ± 0.82	35.94 ± 1.39
heteranthin/1000 μM	6.24 ± 0.90	4.40 ± 0.55	20.93 ± 1.99
heteranthin/500 μM	17.02 ± 1.79	10.78 ± 1.35	34.13 ± 2.01

[a] Data represent mean ± SE of each group.

pounds can modify the oxidant, mutagenic, and carcinogenic effects of some toxicants. Some natural compounds such as quercetin, astaxanthin, and tocopherol have antioxidant and antigenotoxic activities in different kinds of cells.[25,26]

In summary, we isolated two new C-26 and C-30 apocarotenoids, heteranthin (**1**) and ditaxin (**2**), from the hexane-soluble fraction of the seeds of *D. heterantha*. Compounds **1** and **2** exhibited moderate activity in a DPPH• radical scavenging assay and protected the lymphocyte blood cells from genotoxic damage in a dose-dependent manner.

Experimental Section

General Experimental Procedures. Melting points were obtained on an electrothermal melting point apparatus and were uncorrected. Optical rotations were measured on a Perkin-Elmer 241 digital polarimeter at 20 °C. UV spectra were obtained on a Hewlett-Packard 8453 spectrometer. IR spectra were recorded on a Perkin-Elmer Spectrum 2000 Optica FTIR. NMR spectra were recorded on a Varian Mercury 300 spectrometer at 300 MHz for ^{1}H and at 75.4 MHz for ^{13}C, using TMS as internal standard. Mass spectra and HRMS were performed using a Hewlett-Packard 5985-B and a JEOL JMS-AX 505 HA in electron impact (EI) at 70 eV and fast-atom bombardment (FAB) modes, respectively.

Plant Material. *D. heterantha* Zucc. was collected in Totatiche, Jalisco, Mexico, in October 2000. A voucher specimen of the plant is deposited at the Herbarium of the Instituto de Botánica of the Universidad de Guadalajara (IBUG), Jalisco, Mexico (No. 168056).

Extraction and Isolation. The seeds were dehulled manually, and endosperm was ground in a Thomas Wiley 3383-L10 mill and flour was obtained. It was sieved through a number 20 mesh. Hexane (100 mL) was added to 10 g of the ground endosperm, and the mixture was held under constant agitation for 15 min at room temperature under a nitrogen atmosphere, protected from light. The mixture was filtered through Whatman 40 paper, and the residue was extracted a second time. The solvent was evaporated under vacuum at ≤40 °C so that the oil mixed with the pigment could be recovered. To eliminate the fat, the oleoresin was dissolved in acetone in a 1:10 ratio and frozen at −78 °C.[27] Then it was filtered under vacuum using Whatman 40 filter paper that retained solid fat particles. To carry out the transfer of pigments from acetone to petroleum ether, the filtrate was placed in a separatory funnel that contained a mixture of H_2O and petroleum ether and then washed several times with H_2O until the acetone was completely eliminated. The organic layer was dried (Na_2SO_4), and then N_2 was bubbled into the liquid until the solvent was completely evaporated.

After removing the solvent, the residue was purified by open 2.5 × 50 cm column chromatography over Merck (7734) silica gel (200−400 mesh) eluting with Et_2O/petroleum ether, 1:3 v/v, to give seven fractions. Analytical thin-layer chromatography was carried out by using E. Merck silica gel 60 F_{254} coated 0.25 plates. The two major fractions (fractions 4 and 5) were crystallized separately with a mixture of Et_2O/petroleum ether, 1:3, and reprecipitated twice from the same mixture of solvents, to afford the new natural products.

Methyl 3-oxo-12′-apo-ϵ-caroten-12′-oate (1) (heteranthin): yellow, amorphous powder; $[\alpha]^{23}_D$ −669.8 ($CHCl_3$, *c* 0.06); UV−vis (acetone) λ_{max} nm (log ϵ) 237 (5.44), 283 (5.20), 323 (5.02), 359 (4.76), 405 (4.42); R_f 0.65 (Et_2O/petroleum ether, 1:1); mp 120−122 °C (Et_2O/petroleum ether, 1:3); IR (KBr) 1704, 1665, 1543, 1434, 1289, 1233, 1200, 971 cm^{-1}; ^{1}H NMR (300 MHz, $CDCl_3$) and ^{13}C NMR (75.4 MHz, $CDCl_3$), see Tables 1 and 2; MS (70 eV) 394 (M^+, 100), 362 (12), 347 (10), 291 (9), 257 (14), 225 (79), 197 (68), 171 (36), 159 (78), 133 (39), 105 (21), 91 (16), 83 (9); HRMS (FAB, M^+) (*m*NBA) calcd for $C_{26}H_{34}O_3$ 394.2508, found 394.2504.

Methyl 3β,6β-epoxy-5β-hydroxy-4,5-dihydro-8′-apo-ϵ-caroten-8′-oate (2) (ditaxin): orange, amorphous powder; $[\alpha]^{23}_D$ −117.0 ($CHCl_3$, *c* 0.02); UV−vis (acetone) λ_{max} nm (log ϵ) 227 (5.39), 280 (5.20), 322 (5.04), 396 (4.94), 418 (4.93), 459 (4.78); R_f 0.52 (Et_2O/petroleum ether, 1:1); mp 155−156 °C (Et_2O/petroleum ether, 1:3); IR (CH_2Cl_2) 3448, 1702, 1611, 1433, 1385, 1290, 1273, 1232, 1192, 1102, 966 cm^{-1}; ^{1}H NMR (300 MHz, $CDCl_3$) and ^{13}C NMR (75.4 MHz, $CDCl_3$), see Tables 1 and 2; MS (70 eV) 478 (M^+, 6), 398 (9), 277 (35), 221 (29), 197 (22), 181 (46), 135 (30), 95 (23), 91 (30), 43 (100); HRMS (FAB, M^+) (*m*NBA) calcd for $C_{31}H_{42}O_4$ 478.3083, found 478.3084.

Antiradical Activity. The antioxidant activities were determined using DPPH• as a free radical.[28] A 300 μL portion of extract, **1**, **2**, or Trolox (150−1500 μM in MeOH), or lycopene, β-carotene, or astaxanthin (150−1500 μM in Et_2O) was added to a 12 × 75 mm assay tube containing 3 mL of freshly prepared DPPH• solution (150 μM) in MeOH. The tubes were vigorously vortex mixed, covered, and left in the dark at room temperature (~20 °C). After 60 min, the absorbance at 520 nm was measured on a spectrophotometer (Cintra 6 GBC, England). The degree of discoloration of the solution indicates the scavenging efficiency of the added substance. All experiments were performed in triplicate.

Antioxidant activity defined as percent discoloration of DPPH• solution was calculated by the following equation:[29]

$$\mathrm{ARA} = 100 \times (1 - A_{\mathrm{sample}}/A_{\mathrm{control}})$$

where ARA = antioxidant activity, A_{sample} = absorbance of sample after 60 min, and A_{control} = absorbance of control (absence of sample) after 60 min. Data of antioxidant activity were subjected to means comparison by Tukey's test and Pearson correlation according to the statistic program JMP v. 3.0.

Antigenotoxic Activity. Peripheral blood mononuclear cells (PMNC) were isolated from 10 mL samples of whole rat blood, collected into lithium heparin tubes as previously described[30] Briefly, blood was transferred to clean tubes, where an equal volume of cold PBS (pH 7.4) was added and mixed. The buffy coat/PBS mixture was carefully layered onto 3 mL of FICOL histopaque 1077, and after centrifugation at 275*g* and 4 °C for 20 min, the serum/PBS was aspirated and the PMNC transferred into a clean tube and washed twice with PBS (pH 7.4) by spinning at 180*g* for 10 min. Cold PBS was added to the pellet, to a final concentration of 1 × 10^7 cells/mL. The cell viability was counted and checked by trypan blue staining.[31] Cells used in the genotoxicity assay always exceeded 90% viability.

DMSO was used as vehicle for delivering the extracts. The solvents were not found to be toxic to the cells at the concentration used (5%).

The antigenotoxic effect of seed extracts toward lymphocytes was determined by incubating cell suspensions (0.9 mL) with or without seed extracts (0.1 mL) at 37 °C for 30 min and after H_2O_2 to a final concentration of 1 mM at 37 °C for 10 min. Positive controls were prepared by adding H_2O_2 to the cell suspension and negative controls using lymphocytes without any treatment.

The Comet assay was performed under alkaline conditions according to the method of Singh et al.[32] Briefly, 100 μL of cell suspension was mixed in low melting point agarose in phosphate-buffered saline, pH 7.4, and immediately pipetted onto a glass slide precoated with a layer of normal melting point agarose. The agarose was maintained at 4 °C for 5 min to solidify. The third layer of low melting point agarose was added and maintained at 4 °C for 5 min. The slides were immersed in lysing solution (2.5 M NaCl, 100 mM Na_2EDTA, 10 mM Tris, pH 10, 1% sodium sarcocinate, 1% Triton X-100, and 10% DMSO) at 4 °C for 1 h and then placed in a horizontal gel electrophoresis tank containing 300 mM NaOH and 1 mM Na_2EDTA for 40 min before electrophoresis was performed for 15 min using 25 V and 300 mA. The slides were washed with neutralizing buffer (400 mM Tris buffer, pH 7.5) and then stained with etidium bromide.

Slides were placed in a dark humidified chamber at 4 °C to prevent drying of the gel until analysis. Slides were scored using an image analysis system (Meta Systems, Altlussheim, Germany) attached to a fluorescence microscope (Leica, Germany) equipped with appropriate

filters. The microscope was connected to a computer through a charge-coupled device (CCD) camera to transport images to software (Comet Imager) for analysis. The final magnification was 400×. The parameters studied for the cells were the olive tail moment (arbitrary units), tail moment (arbitrary units), and tail length (migration of the DNA from the nucleus; μm). The image analysis software automatically generated the olive tail moment and the tail moment. Images from 50 cells were analyzed.

The data presented are mean ± SE of four values and were analyzed using one-way ANOVA (SAS program). In all cases *p*-values less than 0.05 were considered significant when compared to controls.

Acknowledgment. The authors would like to acknowledge CGPI/IPN (Grant 20040153) and CONACYT-Simorelos 990305012 (Grant: Aprovechamiento Agroindustrial del azafrán de bolita (*D. heterantha*) para la producción de colorantes naturales) for financial support. M.D.M. is grateful to CONACYT for a graduate scholarship. M.E.J. and J.T. are fellows of EDI/IPN and COFAA/IPN.

Note Added after ASAP Publication. The wrong graphic appears for Figure 2 in the version posted on July 22, 2006. The correct Figure 2 appears in the version posted on August 3, 2006. In addition, corrections appear in refs 17, 18, and 27.

References and Notes

(1) Von Lintig, J.; Vogt, K. *J. Biol. Chem*. **2000**, *275*, 11915−11920.
(2) Schwartz, S. H.; Tan, B. C.; Gage, D. A.; Zeevaart, J. A. D.; McCarty, D. R. *Science* **1997**, *276*, 1872−1874.
(3) Enzell, C. *Pure Appl. Chem*. **1985**, *57*, 693−700.
(4) Winterhalter, P.; Straubinger, M. *Food Rev. Int.* **2000**, *16*, 39−59.
(5) Bouvier, F.; Suire, C.; Mutteree, J.; Camara, B. *Science* **2003**, *300*, 2089−2091.
(6) Bouvier, F.; Suire, C.; Mutteree, J.; Camara, B. *Plant Cell* **2003**, *15*, 47−62.
(7) Abdullaev, F. I.; Espinosa-Aguirre, J. J. *Cancer Detect. Prev*. **2004**, *28*, 426−432.
(8) Molnar, P.; Kawase, M.; Satoh, K.; Sohara, Y.; Tanaka, T.; Tani, S.; Sakagami, H.; Nakashima, H.; Motohashi, N.; Gyemant, N.; Molnar, J. *Phytother. Res.* **2005**, *19*, 700−777.
(9) Krinsky, N. I.; Johnson, E. J. *Mol. Aspects Med.* **2005**, *26*, 459−516.
(10) Miller, N. J.; Sampson, J.; Candeias, L. P.; Bramley, P. M.; Rice-Evans, C. A. *FEBS Lett.* **1996**, *384*, 240−242.
(11) Böhm, V.; Puspitasari-Nienaber, N. L.; Ferruzzi, M. G.; Schwartz, S. J. *J. Agric. Food Chem.* **2002**, *50*, 221−226.
(12) Moore, J.; Hao, Z.; Zhou, K.; Luther, M.; Costa, J.; Yu, L. *J Agric. Food Chem.* **2005**, *53*, 6649−6657.
(13) Mortensen, A.; Skibsted, L. H. *J. Agric. Food Chem.* **1997**, *45*, 2970−2977.
(14) Agner, A. R.; Bazo, A. P.; Ribeiro, L. R.; Salvadori, D. M. *Mutat. Res.* **2005**, *582*, 146−154.
(15) Duthie, S. J.; Collins, A. R.; Duthie, G. G.; Dobson, V. L. *Mutat. Res*. **1997**, *393*, 223−231.
(16) Wilms, L. C.; Hollman, C. H.; Boots, A. W.; Kleinjans, C. S. *Mutat Res.* **2005**, *582*, 155−162.
(17) McVaught. Contribution of Michigan Herbarium. In *Flora Nova-Galiciana: A Descriptive Account of the Vascular Plants of Western Mexico*; 1980; Vol. 14, pp 141−152.
(18) Martinez, M. *Catalogo de Nombres Vulgares y Científicos de Plantas Mexicanas*; Botas, Ed.; Fondo de Cultura Economica: México D. F. 1937; p 77.
(19) Mendez-Robles, M. D.; Flores-Chavira,C.; Jaramillo-Flores, M. E.; Orozco-Ávila, I.; Lugo-Cervantes, E. *Econ. Bot.* **2005**, *58*, 530−535.
(20) DellaGreca, M.; Di Marino, C.; Zarrelli, A.; D'Abrosca, B. *J. Nat. Prod.* **2004**, *67*, 1492−1495.
(21) DiMascio, P.; Kaiser, S.; Sies, H. *Arch. Biochem. Biophys.* **1989**, *274*, 532−538.
(22) Nomura, T.; Kikuchi, M.; Kubodera, A.; Kawakami, Y. *Biochem. Mol. Biol. Int.* **1997**, *42*, 361−370.
(23) Gradelet, S.; Leclerc, J.; Siess, M. H.; Astorg, P. O. *Xenobiotica* **1996**, *26*, 909−919.
(24) Krinsky, N. I. *Ann. N.Y. Acad. Sci*. **1998**, *854*, 443−447.
(25) Lyons, N. M.; O'Brien, N. M. *J. Dermatol. Sci.* **2002**, *30*, 73−/84.
(26) Wrona, M.; Anowska, M.; Sarna, T. *Free Radical Biol. Med*. **2004**, *36* (9), 1094−1101.
(27) Rodriguez-Amaya, D. *A Guide to Carotenoid Analysis in Food*; ILSI Press: Washington, 1999; pp 14, 26−28.
(28) Brand-Williams, W.; Cuvelier, M. E.; Berset, C. *Lebensem. Wiss. Technol*. **1995**, *28*, 25−30.
(29) Burda, S.; Oleszek, W. *Agric. Food Chem.* **2001**, *49*, 2774−2779.
(30) Boyum, A. *Scand. J. Clin. Lab. Invest. Suppl.* **1968**, *97*, 77−89.
(31) Kimura, T. *Exp. Hematol. 28*, 6, 635−641.
(32) Singh, N. P.; McCoy, M. T.; Tice, R. R.; Schneider, E. L. *Exp. Cell. Res*. **1988**, *175*, 184−191.

NP050489F